ARTICLE

doi:10.1038/nature10895

Intrinsic coupling of lagging-strand synthesis to chromatin assembly

Duncan J. Smith[1] & Iestyn Whitehouse[1]

Fifty per cent of the genome is discontinuously replicated on the lagging strand as Okazaki fragments. Eukaryotic Okazaki fragments remain poorly characterized and, because nucleosomes are rapidly deposited on nascent DNA, Okazaki fragment processing and nucleosome assembly potentially affect one another. Here we show that ligation-competent Okazaki fragments in *Saccharomyces cerevisiae* are sized according to the nucleosome repeat. Using deep sequencing, we demonstrate that ligation junctions preferentially occur near nucleosome midpoints rather than in internucleosomal linker regions. Disrupting chromatin assembly or lagging-strand polymerase processivity affects both the size and the distribution of Okazaki fragments, suggesting a role for nascent chromatin, assembled immediately after the passage of the replication fork, in the termination of Okazaki fragment synthesis. Our studies represent the first high-resolution analysis—to our knowledge—of eukaryotic Okazaki fragments *in vivo*, and reveal the interconnection between lagging-strand synthesis and chromatin assembly.

During eukaryotic chromosome replication, both genetic and epigenetic information must be accurately duplicated. For chromatin architecture and modifications to be truly epigenetic—that is, heritable despite not being genetically encoded—complete disruption and dissociation of nucleosomes from the replication fork must be prevented to allow the rapid re-deposition of precisely located and appropriately modified histones on the nascent DNA. Histone chaperone complexes govern both nucleosome disassembly and assembly at the replication fork[1].

DNA replication is inherently asymmetric. Okazaki fragment synthesis on the lagging strand necessitates the repeated production of single-stranded DNA and polymerization in the opposite direction to fork progression. Given the delay in lagging-strand synthesis and the rapidity of histone deposition behind the replication fork[2], these two processes may be interlinked. A coordinated series of events occurs each time an Okazaki fragment is synthesized[3]. Each fragment is initiated via an RNA primer[4] and up to 30 nucleotides of DNA, both synthesized by DNA polymerase α (Pol α)-primase[5]; subsequently, the clamp loading factor RFC mediates the replacement of Pol α by the sliding clamp PCNA and the processive polymerase Pol δ (ref. 6). Pol δ extends the nascent DNA chain through the 5′ end of the preceding Okazaki fragment[7,8]; this strand-displacement synthesis generates a 5′ RNA or DNA flap that is cleaved by nucleases such as the flap endonuclease Fen1 (ref. 9). Repeated cycles of extension and DNA cleavage followed by Pol δ idling[10] produce a nick that migrates away from the replication fork and can be sealed by DNA ligase I[11]. Little to no DNA synthesized by the error-prone Pol α remains in the genome after replication[12], suggesting that strand displacement generally replaces at least 30 nucleotides of DNA, but it remains unclear how the replication machinery coordinates the transition from Pol δ to DNA ligase. Indeed, despite their fundamental importance in replication, comparatively little is known about the *in vivo* properties of eukaryotic Okazaki fragments: although they are widely accepted to be shorter than the 1–2 kilobases (kb) observed in prokaryotes, a clear consensus has not emerged[11,13–15]. Moreover, we have little information about how nucleosome assembly may interact with lagging-strand synthesis. A plausible explanation for the difference in size between eukaryotic and prokaryotic Okazaki fragments is that eukaryotic DNA replication occurs within the context of chromatin.

To investigate the relationship between lagging-strand processing and chromatin assembly, we have developed strategies to analyse Okazaki fragments purified from *S. cerevisiae*. We find that Okazaki fragments are heterogeneously sized with a repeat length corresponding to that of nucleosomes. In addition, we find that ligation junctions occur preferentially around known nucleosome midpoints, and that these relationships can be altered by interfering with chromatin assembly or Pol δ processivity. Our data suggest an integrated model whereby nascent chromatin structure facilitates Okazaki fragment processing, which may provide a means to monitor nucleosome assembly behind the replication fork.

Nucleosome-sized Okazaki fragments

To enrich for ligation-competent Okazaki fragments, we constructed strains of *S. cerevisiae* in which DNA ligase I[11] (*CDC9*) expression is driven from a doxycycline-repressible promoter and the encoded protein tagged with a temperature-sensitive degron[16]. The inability to ligate Okazaki fragments should result in the accumulation of nicked DNA that, after purification, can be radiolabelled using DNA polymerase and α-^{32}P dCTP.Ligase inactivation in an asynchronous culture resulted in the accumulation of short heterogeneous DNA species whose abundance increased with duration of ligase inhibition (Fig. 1a). Notably, these fragments displayed an underlying periodicity reminiscent of the nucleosome repeat. Indeed, comparison of the nicked DNA to a nucleosome ladder indicated that a significant fraction of fragments seem to be sized according to the 165-bp nucleosomal repeat length in *S. cerevisiae* (Fig. 1b).

To clarify that we were observing Okazaki fragments, we confirmed that they did not appear in a G1-arrested culture until S-phase release (Fig. 1c). Additionally, we treated purified DNA with recombinant DNA ligase; this repaired the nicks and severely diminished our ability to label fragments (Fig. 1d), showing that our assay predominantly detects nicked DNA rather than species containing single-stranded gaps or flaps resulting from incomplete Okazaki fragment processing. Unrelated control experiments indicated that a 125-nucleotide species previously reported to be Okazaki fragments[14,17] is 5S ribosomal RNA (Supplementary Fig. 2). Thus, we demonstrate that the mono-, di- and

[1]Molecular Biology Program, Memorial Sloan-Kettering Cancer Center, 1275 York Avenue, New York, New York 10065, USA.

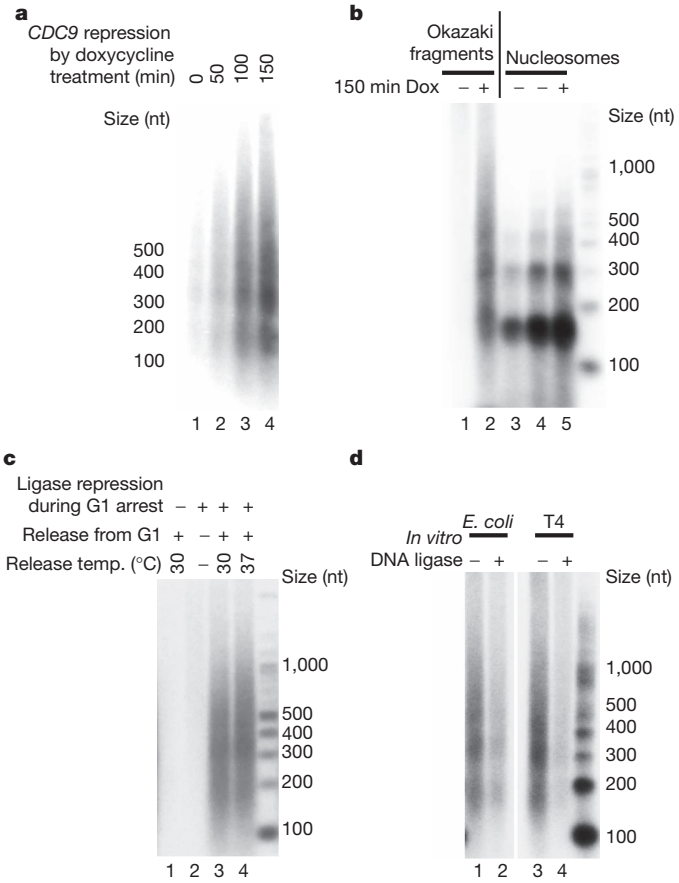

Figure 1 | DNA ligase I depletion in *S. cerevisiae* leads to the accumulation of Okazaki fragments sized similarly to the nucleosome repeat. **a**, Transcriptional repression of DNA ligase I (*CDC9*) results in the accumulation of nicked DNA. Cells carrying a doxycycline-repressible allele of the *CDC9* gene were treated with doxycycline (Dox) for the indicated time. Purified genomic DNA was labelled using exonuclease-deficient Klenow fragment and α-^{32}P dCTP and separated in a denaturing agarose gel. nt, nucleotides. **b**, The size of labelled Okazaki fragments mirrors the nucleosome repeat. Okazaki fragments (lane 2) were labelled as in Fig. 1a; nucleosomes were prepared from wild-type (lane 3) or repressible *CDC9* strains (lanes 4 and 5) by *in vivo* micrococcal nuclease (MNase) digestion. The chromatin digestion patterns in lanes 4 and 5 indicate that *CDC9* repression does not alter global chromatin structure. **c**, Okazaki fragments accumulate during S phase. Cells were arrested in G1 using α-factor, during which time *CDC9* transcription was inhibited by the addition of doxycycline, and degradation of the protein stimulated by activation of the degron system using galactose and 37 °C. Okazaki fragments appear upon release of the culture into S phase (lanes 3 and 4). d, Okazaki fragments are bordered by ligatable nicks. Purified DNA was treated (lanes 2 and 4) or mock-treated (lanes 1 and 3) with the indicated ligase, and then labelled as in Fig. 1a. The inability to label fragments after ligase treatment confirms that labelled Okazaki fragments are flanked by ligatable nicks.

trinucleosome-sized fragments observed on ligase inhibition are generated in S phase and bordered by ligatable nicks—the essential properties of ligation-competent Okazaki fragments.

Global distribution of Okazaki fragments

To explore further the relationship between Okazaki fragments and nucleosomes, we developed a deep sequencing approach to map the strand, position and abundance of fragments across the *S. cerevisiae* genome. To allow yeast to complete S phase in the presence of nicked DNA we inactivated the DNA damage checkpoint by deleting the *RAD9* gene. Additionally, to deplete ligase activity further we deleted the second DNA ligase (*DNL4*). *DNL4* or *RAD9* deletion does not affect Okazaki fragment size (Supplementary Fig. 3). Okazaki fragments were harvested from an asynchronous culture after a ~2.5 h ligase inactivation. Small single-stranded fragments were purified by anion exchange chromatography in alkaline conditions and sequencing primers were ligated directly to each end[18] (Supplementary Fig. 4). Importantly, this method preserves strand identity.

After paired-end deep sequencing, we aligned the data to the *S. cerevisiae* genome and found that use of a single asynchronous culture was sufficient to attain complete coverage (a representative chromosome is shown in Fig. 2a, and a comparison of replicates in Supplementary Fig. 5). Sequencing reads aligning to the Watson or Crick strands showed a complementary distribution with strand bias being particularly pronounced close to replication origins[19]; such asymmetry is expected, given that replication forks proceed bidirectionally from origins (Fig. 2b). The strong strand bias observed around experimentally validated replication origins mapped at high resolution (Fig. 2c)[20] demonstrates preferential sequencing of nascent lagging strands, unequivocally confirming that the DNA species enriched after ligase repression are Okazaki fragments. Detailed analysis of global Okazaki fragment distributions can provide mechanistic insight into replication-fork dynamics (S. McGuffee, D.J.S. and I.W., manuscript in preparation).

Okazaki fragments terminate within nucleosomes

The periodic size of Okazaki fragments observed in Fig. 1 led us to investigate how the ends of Okazaki fragments relate to nucleosome positions found within the yeast genome. We aligned Okazaki fragment termini to a reference list of all consensus nucleosome midpoints (dyads) in *S. cerevisiae*[21]. Inherent bias towards smaller fragments during purification, library amplification and sequencing result in size distributions that differ substantially between starting material and sequenced fragments (Supplementary Fig. 6); therefore, we randomly selected fragments from our sequencing data to approximate the mononucleosome-sized fragments we detected by electrophoresis (Supplementary Fig. 6). Aligning both the 5′ and 3′ ends of mature (Fig. 3a) mononuclesome-sized fragments against the dyads of

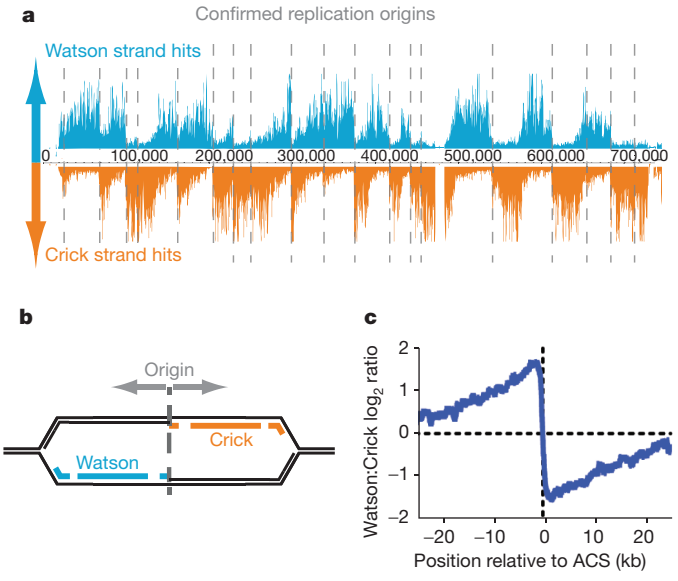

Figure 2 | Sequenced Okazaki fragments show a pronounced bias towards the lagging strand. **a**, Distribution of paired-end sequencing hits mapping to either the Watson (blue, above the axis) or Crick (orange, below) strands across *S. cerevisiae* chromosome 10. The locations of replication origins[19] are indicated as grey dashed lines. Data are unsmoothed. **b**, The anticipated distribution of Okazaki fragments surrounding an efficient origin. **c**, Sequenced Okazaki fragments are strongly enriched in regions predicted to be replicated as the lagging strand. Log_2 ratio of Watson strand: Crick strand fragments across a 50-kb window around ARS consensus sequences (ACS) confirmed previously[20] to correspond to active origins. Data are smoothed to 200 bp.

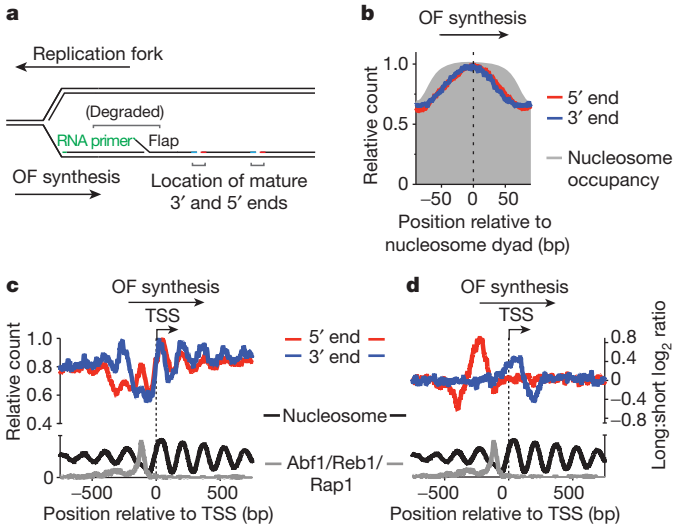

Figure 3 | Okazaki fragment termini are preferentially located at nucleosome dyads. **a**, Schematic indicating the mature Okazaki fragment termini sequenced in this study. **b**, Okazaki fragment termini are enriched around nucleosome dyads. The distribution of termini from mononucleosome-sized Okazaki fragments around the top 50% consensus *S. cerevisiae* nucleosome dyad locations[21] is shown. Unless otherwise indicated, all analyses use unsmoothed data normalized to the maximum signal in the analysed range, and area aligned such that Okazaki fragment (OF) synthesis by Pol δ proceeds from left to right. **c**, The distribution of Okazaki fragment termini correlates with nucleosome occupancy[28] around TSSs. Data are aligned to TSSs such that the direction of transcription is from left to right: only Okazaki fragments synthesized in the same direction as transcription are analysed here; equivalent analyses for fragments synthesized in the opposite direction can be found in Supplementary Fig. 7. Data are smoothed to 5 bp. **d**, Okazaki fragments at nucleosome-depleted regions are disproportionately likely to be long. Equal numbers of reads were selected from the top (long), and the bottom three (short) length quartiles of sequenced fragments. The $\log_2$ ratio of long to short fragments is plotted. Data are smoothed to 5 bp.

high-confidence nucleosomes indicated that the highest density of ends occurs at the dyad (Fig. 3b). Alignment of unfiltered data and dinucleosome-sized fragments is comparable to the mononucleosome size-selected subset (Supplementary Fig. 6). Therefore, rather than being overrepresented in the accessible internucleosomal linker DNA, we find that Okazaki fragment termination is most likely to occur at locations corresponding to nucleosome dyads.

DNA-bound proteins dissociate Pol δ

To confirm that the observed correspondence between nucleosome occupancy and Okazaki fragment end density was not biased by a small subset of nucleosomes, we analysed transcription start sites (TSSs), at which nucleosome positioning follows a well-defined pattern[22]. Alignment of Okazaki fragment termini around ~4,500 TSSs indicated a marked correlation between nucleosome occupancy and the density of Okazaki fragment ends (Fig. 3c and Supplementary Fig. 7) across a broad region surrounding TSSs. Precise nucleosome positioning around TSSs is determined by chromatin remodelling[22,23], allowing us to infer that the correlation refers to remodelled, rather than intrinsically preferred, nucleosome locations.

If the ends of Okazaki fragments are dictated by nucleosomes then nicks should always be in register with positioned nucleosomes, regardless of internucleosomal spacing. Thus, nucleosomes separated by long linker DNA should be associated with longer Okazaki fragments. We took advantage of the differential nucleosome spacing surrounding the nucleosome-depleted region (NDR) at TSSs, comparing the distribution of equal numbers of randomly selected long and short fragments (defined, respectively, as the top quartile of sequenced fragments by length, and the bottom three quartiles). When the ratio of long to short fragments is plotted across this region (Fig. 3d and Supplementary Fig. 7), we find that fragments whose ends map within nucleosomes bordering the NDR are disproportionately long. Thus, Okazaki fragment length reflects nucleosome spacing.

As well as correlating with nucleosome occupancy, Okazaki fragment termini were enriched around known transcription factor binding sites (Fig. 3c)[24,25]. This suggested that, in addition to nucleosomes, sequence-specific DNA binding factors might directly influence the ends of Okazaki fragments. Such correlations would be expected if, following replication-fork passage, some transcription factors rapidly bound to replicated DNA and impeded Pol δ during strand-displacement synthesis, causing the polymerase to dissociate and leave a nick close to the site of collision. Furthermore, this model would also provide an explanation for the observed link between nucleosome occupancy and Okazaki fragment termination: nucleosomes contain numerous weak protein–DNA interactions, whose cumulative strength peaks around the dyad[26]. Polymerases can invade nucleosomes, but experience increasing resistance as they approach the dyad[27,28]. Therefore, if nucleosomes are rapidly re-established on the lagging strand behind the replication fork, and Pol δ invades them during strand-displacement synthesis, the likelihood of polymerase stalling and/or dissociation will increase with proximity to the dyad (see model in Supplementary Fig. 1), producing Okazaki fragments sized according to the nucleosome repeat. Other models that invoke biased Okazaki fragment initiation due to replisome pausing on encountering nucleosomes would produce distinct correlations around NDRs (Supplementary Fig. 8).

If polymerization by Pol δ is inhibited by sequence-specific DNA-bound transcription factors, Okazaki fragment ends should accumulate on the side of the factor that is first encountered by Pol δ. Aligning all transcription factor binding sites[25] indicated a significant enrichment of precisely juxtaposed Okazaki fragment 5′ and 3′ termini around the replication-fork-proximal side of the binding site (Fig. 4a). However, when the Abf1, Reb1 and Rap1 binding sites were considered separately we found that, among transcription factors, these proteins most strongly biased the positioning of Okazaki fragment ends (Fig. 4b, c and Supplementary Fig. 9). Abf1, Reb1 and Rap1 have essential roles in chromatin organization[24,29], and may therefore bind more rapidly and tightly to newly replicated DNA than the majority of transcription factors. We observed a strand-dependent enrichment of Okazaki fragment termini around the 3′ ends of tRNA genes, as well as transcription factor TFIIIB binding sites (Supplementary Fig. 10). Thus, it seems that diverse DNA binding proteins can influence the processing of Okazaki fragments and probably facilitate the dissociation of Pol δ, with tightly bound protein complexes stimulating termination more precisely than those, such as nascent histones, that have more diffuse binding regions.

Chromatin assembly dictates nick location

Two testable predictions arise from the model that Pol δ dissociates via interaction with nascent nucleosomes: (1) disrupting nucleosome

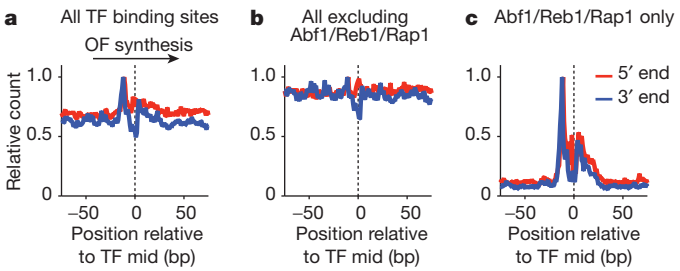

Figure 4 | Transcription factors with roles in nucleosome positioning stimulate dissociation of Pol δ. **a**, Okazaki fragment termini are enriched on the replication-fork-proximal side of known transcription factor (TF) binding sites[25]. Mid, midpoint of TF binding site. **b**, **c**, The enrichment of Okazaki fragment termini around transcription factor binding sites can be attributed almost entirely to three factors—Abf1, Reb1 and Rap1—known to have roles in nucleosome positioning.

assembly will impair nucleosome-mediated Okazaki fragment termination and should, therefore, alter the size distribution of the fragments; and (2) reducing Pol δ processivity will result in a shift of Okazaki fragment termination sites away from the dyad, towards the replication-fork-proximal side of nucleosomes.

The deposition of $(H3H4)_2$ tetramers on nascent DNA—the first stage in nucleosome assembly—is mediated in part by CAF-1, a multisubunit histone chaperone complex associated with the replisome via PCNA[30]. We deleted each subunit of CAF-1 individually, and compared the length of Okazaki fragments in the deletion strains to those with wild-type CAF-1 (Fig. 5a). Loss of any CAF-1 subunit abrogated the periodic sizing of Okazaki fragments, significantly increasing their average length. These data are consistent with a global delay in $(H3H4)_2$ deposition following replication, with the resulting paucity of tetrasomes/nucleosomes on the lagging strand leading to increased strand displacement by Pol δ and thus to longer Okazaki fragments.

In *S. cerevisiae*, Pol δ is a heterotrimer whose Pol32 subunit increases processivity and PCNA binding affinity[31]; Pol δ lacking Pol32 shows decreased strand-displacement synthesis *in vitro* and probably *in vivo*[32]. Labelled Okazaki fragments from a *pol32*Δ strain were more heterogeneous but were still generally sized according to the nucleosome repeat (Fig. 5b). When the positions of the 5′ and 3′ termini of mononucleosome-sized fragments (165 ± 15 nucleotides, as per Fig. 3b) from the *pol32*Δ strain were aligned against nucleosome midpoints, a clear shift was observed towards the first edge of the nucleosome encountered by the polymerase (Fig. 5c and Supplementary Fig. 11). Therefore, when Pol δ processivity is perturbed, the polymerase dissociates more rapidly due to an inability to invade nascent nucleosomes assembled on Okazaki fragments. The new maximum end density occurs ~35–40 nucleotides from the dyad, consistent with the extent of DNA protected by $(H3H4)_2$ tetramers[33]: nucleosome assembly occurs step-wise, with assembly of $(H3H4)_2$ tetramers preceding recruitment of H2A/H2B[34]; it is therefore possible that the histone–DNA species encountered by Pol δ is a tetrasome rather than a nucleosome, although our data do not allow us to distinguish between these possibilities. Importantly, the distribution of Okazaki fragment termini around transcription factor binding sites was identical between wild-type and *pol32*Δ strains (Supplementary Fig. 9), allowing us to conclude that the shift towards the edge of nucleosomes does not simply represent a constant decrease of ~35–40 bp in the extent of strand displacement.

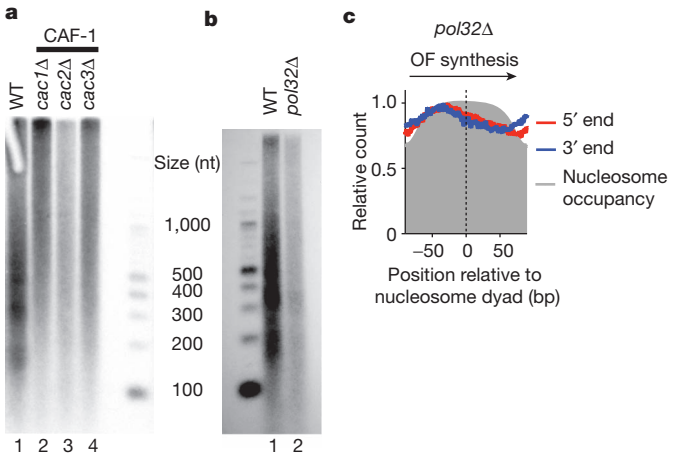

Figure 5 | Impaired chromatin assembly and Pol δ processivity affect the size of Okazaki fragments and the location of their termini, respectively. **a**, Deletion of any component of the CAF-1 complex (lanes 2–4) results in Okazaki fragments that are no longer sized according to nucleosomes. WT, wild type. **b**, Deletion of the *pol32* subunit of Pol δ (lane 2) does not abrogate the chromatin-like size distribution of Okazaki fragments. **c**, In the absence of Pol32, the termini of mononucleosome-sized Okazaki fragments are shifted towards the replication-fork-proximal edge of the nucleosome: peak density occurs at a location consistent with the predicted edges of $(H3H4)_2$ tetramers. See also Supplementary Fig. 11.

Discussion

Our data suggest a mechanism by which Pol δ may reliably remove DNA synthesized by Pol α while avoiding excessive strand-displacement synthesis. Repeated cycles of extension and cleavage can occur during the synthesis of a single Okazaki fragment. After removal of the RNA primer, all DNA flap structures generated by Pol δ are biochemically indistinguishable from one another, and an external mechanism is therefore required to measure the extent of strand displacement already carried out by Pol δ on each fragment. The removal of Pol δ by newly deposited histones represents a simple way to constrain Pol δ extension, and might allow nucleosome assembly to stimulate replication-fork progression directly. Although our data imply that nucleosomes strongly impede Pol δ, we note that both Fen1 and DNA ligase I can act efficiently on nucleosomal substrates[35,36]. We speculate that carrying out Okazaki fragment processing in the context of nucleosomes rather than DNA allows the ligation reaction to outcompete further strand displacement by Pol δ.

CAF-1 is not essential in *S. cerevisiae*, suggesting that other histone chaperones such as Asf1, Rtt106 and HIR[37] allow sufficient replication-coupled or post-replicative nucleosome assembly for viability. Nevertheless, our results are consistent with a temporal delay in nucleosome assembly in CAF-1 mutants, which may give rise to previously reported silencing defects[38]. The importance of replication-coupled chromatin assembly in metazoa is illustrated by the severe phenotypes of CAF-1 or ASF1 disruption in human cell lines: ASF1 depletion leads to replication-fork stalling[39], and CAF-1 depletion also precludes progression through S phase[40].

Our studies demonstrate that the location of Okazaki fragment termini can be determined by interactions between the lagging-strand polymerase and nascent nucleosomes. This observation provides the first direct mechanistic evidence for the coupling of DNA replication to chromatin assembly on the newly replicated daughter genomes. Such coupling is fundamentally important given the part played by chromatin in the regulation of gene expression, as well as the potential for the epigenetic inheritance of precisely located modified nucleosomes. In addition, transcription factors known to have roles in the establishment of chromatin structure are apparently able to re-bind to DNA immediately after replication-fork passage. Unlike histones, which are present in sufficient number to be distributed to both daughter genomes, DNA-bound transcription factors are present at only one local copy per two daughters. Regulation of transcription factor re-binding could thus have a key role in asymmetric epigenetic inheritance.

METHODS SUMMARY

Genomic DNA was prepared from spheroblasts essentially as described for medium resolution DSB mapping[41], labelled using exo-Klenow fragment (NEB) and α-^{32}P dCTP and separated in 1.3% denaturing agarose gels.

Okazaki fragments were purified by binding heat-denatured genomic DNA to Source 15Q (GE Healthcare) at pH 12, 300 mM NaCl, and eluting in 50 mM steps to 1 M. Primers for paired-end Illumina TruSeq sequencing were directly ligated to each end. Following second-strand synthesis and size selection by gel purification, libraries were amplified by PCR, purified from two sequential 2.5% native agarose gels, and sequenced directly. Full details are in Supplementary Fig. 4 and Methods.

Full Methods and any associated references are available in the online version of the paper at www.nature.com/nature.

Received 21 November 2011; accepted 24 January 2012.
Published online 14 March 2012.

1. Corpet, A. & Almouzni, G. Making copies of chromatin: the challenge of nucleosomal organization and epigenetic information. *Trends Cell Biol.* **19,** 29–41 (2009).

2. Sogo, J. M., Stahl, H., Koller, T. & Knippers, R. Structure of replicating simian virus 40 minichromosomes. The replication fork, core histone segregation and terminal structures. *J. Mol. Biol.* **189,** 189–204 (1986).
3. Burgers, P. M. Polymerase dynamics at the eukaryotic DNA replication fork. *J. Biol. Chem.* **284,** 4041–4045 (2009).
4. Kaufmann, G. & Falk, H. H. An oligoribonucleotide polymerase from SV40-infected cells with properties of a primase. *Nucleic Acids Res.* **10,** 2309–2321 (1982).
5. Nethanel, T. & Kaufmann, G. Two DNA polymerases may be required for synthesis of the lagging DNA strand of simian virus 40. *J. Virol.* **64,** 5912–5918 (1990).
6. Waga, S. & Stillman, B. Anatomy of a DNA replication fork revealed by reconstitution of SV40 DNA replication *in vitro*. *Nature* **369,** 207–212 (1994).
7. Ayyagari, R., Gomes, X. V., Gordenin, D. A. & Burgers, P. M. Okazaki fragment maturation in yeast. I. Distribution of functions between FEN1 and DNA2. *J. Biol. Chem.* **278,** 1618–1625 (2003).
8. Bae, S. H., Bae, K. H., Kim, J. A. & Seo, Y. S. RPA governs endonuclease switching during processing of Okazaki fragments in eukaryotes. *Nature* **412,** 456–461 (2001).
9. Kao, H. I., Veeraraghavan, J., Polaczek, P., Campbell, J. L. & Bambara, R. A. On the roles of *Saccharomyces cerevisiae* Dna2p and Flap endonuclease 1 in Okazaki fragment processing. *J. Biol. Chem.* **279,** 15014–15024 (2004).
10. Garg, P., Stith, C. M., Sabouri, N., Johansson, E. & Burgers, P. M. Idling by DNA polymerase δ maintains a ligatable nick during lagging-strand DNA replication. *Genes Dev.* **18,** 2764–2773 (2004).
11. Johnston, L. H. & Nasmyth, K. A. *Saccharomyces cerevisiae* cell cycle mutant *cdc9* is defective in DNA ligase. *Nature* **274,** 891–893 (1978).
12. Pavlov, Y. I. *et al.* Evidence that errors made by DNA polymerase α are corrected by DNA polymerase δ. *Curr. Biol.* **16,** 202–207 (2006).
13. Anderson, S. & DePamphilis, M. L. Metabolism of Okazaki fragments during simian virus 40 DNA replication. *J. Biol. Chem.* **254,** 11495–11504 (1979).
14. Bielinsky, A. K. & Gerbi, S. A. Discrete start sites for DNA synthesis in the yeast *ARS1* origin. *Science* **279,** 95–98 (1998).
15. Blumenthal, A. B. & Clark, E. J. Discrete sizes of replication intermediates in *Drosophila* cells. *Cell* **12,** 183–189 (1977).
16. Dohmen, R. J. & Varshavsky, A. Heat-inducible degron and the making of conditional mutants. *Methods Enzymol.* **399,** 799–822 (2005).
17. Bielinsky, A. K. & Gerbi, S. A. Chromosomal *ARS1* has a single leading strand start site. *Mol. Cell* **3,** 477–486 (1999).
18. Ng, P. *et al.* Gene identification signature (GIS) analysis for transcriptome characterization and genome annotation. *Nature Methods* **2,** 105–111 (2005).
19. Nieduszynski, C. A., Hiraga, S., Ak, P., Benham, C. J. & Donaldson, A. D. OriDB: a DNA replication origin database. *Nucleic Acids Res.* **35,** D40–D46 (2007).
20. Eaton, M. L., Galani, K., Kang, S., Bell, S. P. & MacAlpine, D. M. Conserved nucleosome positioning defines replication origins. *Genes Dev.* **24,** 748–753 (2010).
21. Jiang, C. & Pugh, B. F. A compiled and systematic reference map of nucleosome positions across the *Saccharomyces cerevisiae* genome. *Genome Biol.* **10,** R109 (2009).
22. Whitehouse, I., Rando, O. J., Delrow, J. & Tsukiyama, T. Chromatin remodelling at promoters suppresses antisense transcription. *Nature* **450,** 1031–1035 (2007).
23. Hartley, P. D. & Madhani, H. D. Mechanisms that specify promoter nucleosome location and identity. *Cell* **137,** 445–458 (2009).
24. Badis, G. *et al.* A library of yeast transcription factor motifs reveals a widespread function for Rsc3 in targeting nucleosome exclusion at promoters. *Mol. Cell* **32,** 878–887 (2008).
25. MacIsaac, K. D. *et al.* An improved map of conserved regulatory sites for *Saccharomyces cerevisiae*. *BMC Bioinformatics* **7,** 113 (2006).
26. Hall, M. A. *et al.* High-resolution dynamic mapping of histone–DNA interactions in a nucleosome. *Nature Struct. Mol. Biol.* **16,** 124–129 (2009).
27. Bondarenko, V. A. *et al.* Nucleosomes can form a polar barrier to transcript elongation by RNA polymerase II. *Mol. Cell* **24,** 469–479 (2006).
28. Churchman, L. S. & Weissman, J. S. Nascent transcript sequencing visualizes transcription at nucleotide resolution. *Nature* **469,** 368–373 (2011).
29. Bai, L., Ondracka, A. & Cross, F. R. Multiple sequence-specific factors generate the nucleosome-depleted region on *CLN2* promoter. *Mol. Cell* **42,** 465–476 (2011).
30. Shibahara, K. & Stillman, B. Replication-dependent marking of DNA by PCNA facilitates CAF-1-coupled inheritance of chromatin. *Cell* **96,** 575–585 (1999).
31. Johansson, E., Garg, P. & Burgers, P. M. The Pol32 subunit of DNA polymerase δ contains separable domains for processive replication and proliferating cell nuclear antigen (PCNA) binding. *J. Biol. Chem.* **279,** 1907–1915 (2004).
32. Stith, C. M., Sterling, J., Resnick, M. A., Gordenin, D. A. & Burgers, P. M. Flexibility of eukaryotic Okazaki fragment maturation through regulated strand displacement synthesis. *J. Biol. Chem.* **283,** 34129–34140 (2008).
33. Dong, F. & van Holde, K. E. Nucleosome positioning is determined by the (H3–H4)2 tetramer. *Proc. Natl Acad. Sci. USA* **88,** 10596–10600 (1991).
34. Smith, S. & Stillman, B. Stepwise assembly of chromatin during DNA replication *in vitro*. *EMBO J.* **10,** 971–980 (1991).
35. Chafin, D. R., Vitolo, J. M., Henricksen, L. A., Bambara, R. A. & Hayes, J. J. Human DNA ligase I efficiently seals nicks in nucleosomes. *EMBO J.* **19,** 5492–5501 (2000).
36. Huggins, C. F. *et al.* Flap endonuclease 1 efficiently cleaves base excision repair and DNA replication intermediates assembled into nucleosomes. *Mol. Cell* **10,** 1201–1211 (2002).
37. Ray-Gallet, D. *et al.* Dynamics of histone H3 deposition *in vivo* reveal a nucleosome gap-filling mechanism for H3.3 to maintain chromatin integrity. *Mol. Cell* **44,** 928–941 (2011).
38. Zhang, Z., Shibahara, K. & Stillman, B. PCNA connects DNA replication to epigenetic inheritance in yeast. *Nature* **408,** 221–225 (2000).
39. Groth, A. *et al.* Regulation of replication fork progression through histone supply and demand. *Science* **318,** 1928–1931 (2007).
40. Hoek, M. & Stillman, B. Chromatin assembly factor 1 is essential and couples chromatin assembly to DNA replication *in vivo*. *Proc. Natl Acad. Sci. USA* **100,** 12183–12188 (2003).
41. Murakami, H., Borde, V., Nicolas, A. & Keeney, S. Gel electrophoresis assays for analyzing DNA double-strand breaks in *Saccharomyces cerevisiae* at various spatial resolutions. *Methods Mol. Biol.* **557,** 117–142 (2009).

Supplementary Information is linked to the online version of the paper at www.nature.com/nature.

Acknowledgements We thank S. McGuffee for assistance with data processing; S. Keeney, K. Marians, D. Remus, T. Tsukiyama, members of the Molecular Biology Program and Whitehouse laboratory for discussions and comments on the manuscript. This work was supported by a Louis V. Gerstner Jr Young Investigator Award and an Alfred Bressler Scholars Endowment Award to I.W. D.J.S. is an HHMI fellow of the Damon Runyon Cancer Research Foundation (DRG-#2046-10).

Author Contributions D.J.S. and I.W. designed experiments; D.J.S. performed experiments and analysed data; D.J.S. and I.W. interpreted results; the manuscript was drafted by D.J.S. and edited by D.J.S. and I.W.

Author Information Raw sequencing data and processed data are available at the Gene Expression Omnibus (http://www.ncbi.nlm.nih.gov/geo/query/acc.cgi?acc=GSE33786) under accession number 33786. Reprints and permissions information is available at www.nature.com/reprints. The authors declare no competing financial interests. Readers are welcome to comment on the online version of this article at www.nature.com/nature. Correspondence and requests for materials should be addressed to I.W. (whitehoi@mskcc.org).

METHODS

DNA purification. Yeast strains carrying degron-tagged, doxycycline-repressible alleles of *CDC9* and a galactose-inducible *UBR1* allele (see Supplementary Table 1 for a list of strains) were grown at 30 °C in YEP supplemented with 2% raffinose. At optical density (OD) 0.4, galactose and doxycycline were added to final concentrations of 2% and 40 mg l^{-1}, respectively, and the culture shaken at 37 °C for 2.5 h. Fifty-millilitre cultures were used for labelling experiments, and 250-ml cultures for purification and library generation.

Genomic DNA was prepared from spheroblasts as described for medium resolution DSB mapping[41]. Following ligase repression, cells were collected by centrifugation, washed in SCE buffer (1 M sorbitol, 100 mM sodium citrate, 60 mM EDTA, pH 7.0) and spheroblasted for 3 min with 5 mg zymolyase 20T (USB) per 50-ml culture. Spheroblasts were washed with SCE, and resuspended in 480 µl lysis buffer (50 mM Tris-HCl, pH 8.0, 50 mM EDTA, 100 mM NaCl, 1.5% sarkosyl) containing 150 µg proteinase K (Fisher). Digestion was carried out for 2–16 h at 37 °C. After digestion, residual proteins and peptides were precipitated by adding 200 µl 5 M KOAc and spinning at 16,000*g* for 30 min at 4 °C. Nucleic acids were precipitated from the supernatant by addition of 500 µl isopropanol and centrifugation at 16,000*g* for 10 min. Pellets were washed twice with 500 µl 70% ethanol, resuspended in 200 µl STE buffer (10 mM Tris-HCl, pH 8.0, 1 mM EDTA, 100 mM NaCl) and digested with 25 µg RNase A (Sigma) and/or 10 U RIboshredder RNase blend (Epicentre) at 37 °C for 30 min. Genomic DNA was precipitated by addition of 20 µl NaOAc, pH 5.5 and 800 µl ethanol followed by centrifugation at 5,000*g* for 10 min at room temperature (25 °C). Pellets were washed with 70% ethanol and resuspended in 1 µl TE (10 mM Tris:Cl pH 7.5, 0.1 mM EDTA) per ml original culture volume. DNA was stored at 4 °C and never frozen.

DNA labelling. Two microlitres of DNA (corresponding to the genomic DNA content of 2 ml cultured cells) was used in 20 µl labelling reactions containing 5 U Klenow (exo-)polymerase (NEB) and α-dCTP (Perkin Elmer) at a final concentration of 33 nM. Free label was removed using Illustra microspin G-50 columns (GE healthcare). Labelled DNA was separated in 1.3% denaturing agarose gels (50 mM NaOH, 1 mM EDTA). After electrophoresis, the gel was neutralized and DNA transferred to an uncharged nitrocellulose membrane (Hybond-N; GE healthcare) via capillary transfer. Membranes were exposed to phosphor screens or film.

Okazaki fragment purification. Genomic DNA purified as described earlier was denatured by heating to 95 °C for 5 min, rapidly cooled on ice and brought to 300 mM NaCl, pH 12. Purification was carried out in batch using 400 µl Source 15Q (GE healthcare), binding at 300 mM NaCl, pH 12 and eluting in 50 mM steps to 1 M NaCl, pH 12. As determined by purification of fragments pre-labelled as above (see also Supplementary Fig. 4), fractions from 800–900 mM NaCl contained the majority of fragments of interest. DNA was ethanol precipitated and treated with 10 U Riboshredder RNase blend for 30 min at 37 °C to remove residual, undigested RNA: digestion products were removed using Illustra microspin G-50 columns to leave essentially pure Okazaki fragments.

Sequencing library generation. Adaptor primer pairs with single-stranded overhangs (shown schematically in Supplementary Fig. 4) were annealed by cooling from 95 °C and purified from 12% native polyacrylamide gels via standard methods. Sequences of the adaptor pairs are as follows. 5′ top, ACACTCTTTCCCTACACG ACGCTCTTCCGATCT; 5′ bottom, NNNNNNAGATCGGAAGAGCGTCGTGT AGGGAAAGAGTGT; 3′ top, /Phos/AGATCGGAAGAGCGGTTCAGCAGGAA TGCCGAG; 3′ bottom, CTCGGCATTCCTGCTGAACCGCTCTTCCGATCTN NNNNN.

Up to 200 ng denatured purified Okazaki fragments were incubated at 16 °C overnight in a ligation reaction containing 1 µg of each primer pair and 1,000 U T4 DNA ligase (NEB). Unligated adaptors were removed using Illustra microspin S-300 columns (GE healthcare) and a second strand-synthesis reaction carried out at 72 °C using Taq polymerase (NEB). Products from ~200–1,000 bp were purified from 2.5% agarose gels run in TBE using Qiaquick kits (Qiagen). Purified libraries were amplified (16 cycles) using Illumina Truseq primers according to Illumina protocols, except that KOD hot start polymerase (Novagen) was used. Amplified libraries were purified from two sequential 2.5% agarose gels. Subsequent steps in the sequencing workflow were carried out according to standard procedures.

Nucleosome dyad and occupancy data. The top 50% of nucleosome dyads (by confidence score), taken from a meta-analysis[21], were used in our analysis; nucleosome occupancy data (Fig. 3b) were from the YPD data set detailed previously[42].

42. Kaplan, N. *et al.* The DNA-encoded nucleosome organization of a eukaryotic genome. *Nature* **458,** 362–366 (2009).